

THE 1989 EARTHQUAKE SWARM BENEATH MAMMOTH MOUNTAIN, CALIFORNIA: AN INITIAL LOOK AT THE 4 MAY THROUGH 30 SEPTEMBER ACTIVITY

BY D. P. HILL, W. L. ELLSWORTH, M. J. S. JOHNSTON, J. O. LANGBEIN,
D. H. OPPENHEIMER, A. M. PITT, P. A. REASENBERG, M. L. SOREY,
AND S. R. MCNUTT

ABSTRACT

Mammoth Mountain is a 50,000- to 200,000-year-old cumulo volcano standing on the southwestern rim of Long Valley in eastern California. On 4 May 1989, two $M = 1$ earthquakes beneath the south flank of the mountain marked the onset of a swarm that has continued for more than 6 months. In addition to its longevity, noteworthy aspects of this persistent swarm include (1) an exponential-like increase in the rate of activity through the first month; (2) a vertically oriented, planar distribution of hypocenters at depths between 6 and 9 km with a north-northeast strike (roughly perpendicular to the average T -axis orientation for the swarm earthquakes); (3) recurring spasmodic bursts (rapid-fire sequences of similar-sized earthquakes with overlapping coda) and occasional earthquakes with enhanced low-frequency energy; (4) a uniform temporal distribution of the four largest ($M \approx 3$) events over the first 4 months of the swarm with a cumulative seismic moment for the entire sequence through 30 September corresponding to a single $M \approx 4$ earthquake; (5) a b -value of 1.2; and (6) submicrostrain perturbations on the nearby borehole dilatometer, the first of which led the onset of swarm activity by more than 2 weeks. These aspects of the swarm, together with its location along the southern extension of the youthful Mono-Inyo volcanic chain, which last erupted 500 to 600 years ago, point to a magmatic source for the modest but persistent influx of strain energy into the crust beneath Mammoth Mountain.

INTRODUCTION

On 4 May 1989, two $M \approx 1$ earthquakes occurred beneath Mammoth Mountain on the southwestern rim of Long Valley caldera (Fig. 1) heralding the onset of a swarm of small ($M < 3.2$) earthquakes beneath the mountain that has persisted for at least 6 months. This is not the first swarm to occur under Mammoth Mountain since the dense seismic and deformation networks became operational in Long Valley caldera in mid-1982, but it has certainly sustained a higher activity rate for a much longer time than any of the earlier swarms. In this paper, we summarize some initial observations on the swarm based on preliminary analyses of data through the end of September from the seismic and deformation networks designed to monitor unrest in Long Valley caldera. As more thorough analyses of individual data sets are completed, we expected unresolved details in this preliminary analysis to come into sharper focus.

BACKGROUND

Mammoth Mountain is a cumulo volcano constructed of rhyolite and quartz latite lavas erupted between 200,000 and 50,000 years ago (Bailey, 1989). Its growth postdates the caldera-forming eruption of the Bishop tuff 730,000 years ago and brackets the last eruption from the residual Long Valley magma chamber in the west moat of the caldera 100,000 years ago (Bailey, 1989). Activity along the more

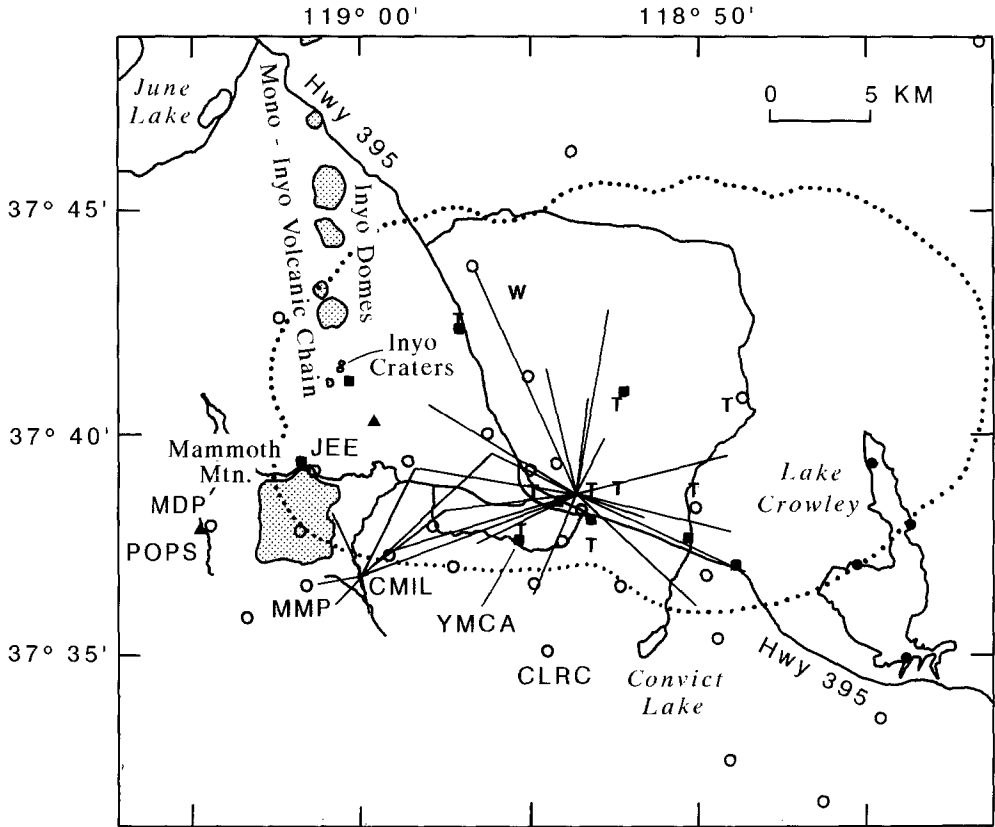


FIG. 1. Map showing location of Mammoth Mountain and principal monitoring networks in Long Valley caldera. Dotted line indicates caldera boundary. O, seismometer; T, tiltmeter; W, water well; Δ , Dilatometer; —, two-color geodimeter; L, level array.

youthful Mono-Inyo volcanic chain (Fig. 1) began about 40,000 years ago with the most recent eruptions occurring 500 to 600 years ago from several vents along the north end of the Mono Craters and the south end of the Inyo craters (Miller, 1985; Sieh and Bursik, 1986). Mammoth Mountain lies along the southern extension of the Mono-Inyo volcanic chain, and several small explosion craters on the north flank of the mountain were produced by phreatic (steam-blast) eruptions associated with the intrusion of the silicic dike that produced the Inyo Dome eruptions, the Inyo Craters phreatic eruptions, and the series of grabens and fractures that include the "Earthquake Fault" (Bailey, 1989; Miller, 1985). The Red Cones, 4 km southwest of Mammoth Mountain, lie further south along this same trend. These postglacial, basaltic cinder cones are roughly 5000 years old (D. Miller, personal comm., 1989).

Numerous papers document the repeated earthquake swarms and 50 cm uplift of the central section of the caldera floor in Long Valley caldera and vicinity during the last decade (see summaries by Hill *et al.*, 1985; and Rundle and Hill, 1988). Principal events in this unrest include a $M = 5.8$ earthquake 15 km southeast of the caldera on 4 October 1978, four $M \approx 6$ events near the southern margin of the caldera on 25 to 27 May 1980, followed by repeated $M \approx 4$ swarms in the south moat of the caldera through mid 1982, an intense earthquake swarm in the south moat with two $M = 5.3$ earthquakes in January 1983, a $M = 5.8$ earthquake 20 km southeast of the caldera on 23 November 1984, and a $M = 6.4$ earthquake

25 km east southeast of the caldera on 21 July 1986. Roughly half (25 cm) of the uplift of the caldera floor (resurgent dome) occurred sometime between mid-1979 and mid-1980 (Savage and Clark, 1980); the remaining 25 cm has accumulated at a slowly decaying rate from 1983 to the present.

PREVIOUS MAMMOTH MOUNTAIN ACTIVITY

The catalogs for instrumentally recorded earthquakes in California and western Nevada indicate that, while the section of the Sierra Nevada escarpment immediately south of Long Valley caldera has been one of the most persistent sources of $M = 4$ to 6 earthquakes in California this century, the crust beneath Mammoth Mountain itself is essentially aseismic at this magnitude level. The regional seismic networks established by the California Institute of Technology (Hileman *et al.*, 1973) and the University of California, Berkeley, (Bolt and Miller, 1975) in the early 1930s, however, did not have the capability of detecting $M \leq 3$ earthquakes in the region until the mid 1950s. Stations added to the University of Nevada, Reno, seismic network in the late 1970s further improved coverage so that by 1979 the detection threshold for earthquakes occurring in the vicinity of Long Valley caldera was close to $M \approx 2$ (Smith and Ryall, 1980). No $M \geq 2$ earthquakes were located beneath Mammoth Mountain by temporary seismic networks operated in the area during October 1970 and May 1972 (Pitt and Steeples, 1975; Steeples and Pitt, 1975) and from mid-1979 through mid-1980 (Cramer and Toppazada, 1980). Steeples and Pitt (1975), however, report a swarm of 10 ($M \leq 2.5$) events 3 km southeast of the mountain during the May 1972 recording session. Thus, swarms of small ($M < 3$) earthquakes beneath Mammoth Mountain may have gone undetected up through the mid to late 1970s, but it appears that the mountain was indeed seismically quiet from 1979 through mid-1982.

The record of $M \geq 1.2$ earthquakes is essentially complete after mid-1982 when the first 16 stations of the telemetered seismic network in Long Valley caldera became operational. Hypocentral locations for earthquakes occurring beneath the caldera and Mammoth Mountain obtained from the network, which currently includes 22 stations within and immediately adjacent to the caldera (Fig. 1), have a precision of about ± 0.5 km in the horizontal dimension and ± 1 km in depth. Figure 2 shows the time history of $M \geq 1.2$ earthquakes beneath Mammoth Mountain (events within the box $37^{\circ}35'$ to $37^{\circ}40'N$ and from $119^{\circ}00'$ to $119^{\circ}10'W$) since June 1982. Occasional swarms of small ($M < 3.5$) earthquakes began occurring beneath the mountain in mid-1982 only to slowly die away beginning in mid-1984. Relative quiescence with occasional $M \leq 2$ events persisted from late 1985 until the onset of the current swarm in May 1989. Activity from mid-1982 to 1985 occurred in brief swarms of $M \leq 3$ events that lasted only a few hours to a day or two. Two $M = 3$ events occurred during this initial interval; one on 15 September 1983 and the other on 5 February 1984. The latter was unique for Mammoth Mountain activity in that it occurred as a mainshock followed by several days of smaller aftershocks rather than in a swarm-like sequence. The activity rate during this 1982 to 1985 period averaged about four $M > 1.2$ earthquakes per month.

Epicenters of the swarm earthquakes during the 1982 to 1985 period define four irregularly shaped clusters beneath the flanks of the mountain with relatively few events beneath the summit (Fig. 3a). The sparse cluster beneath the southwest flank outlines the location of the most intense activity in the current swarm. The corresponding hypocenters occupy a tabular volume of the crust approximately 2 km thick that dips steeply to the south-southwest from depths of less than 4 km

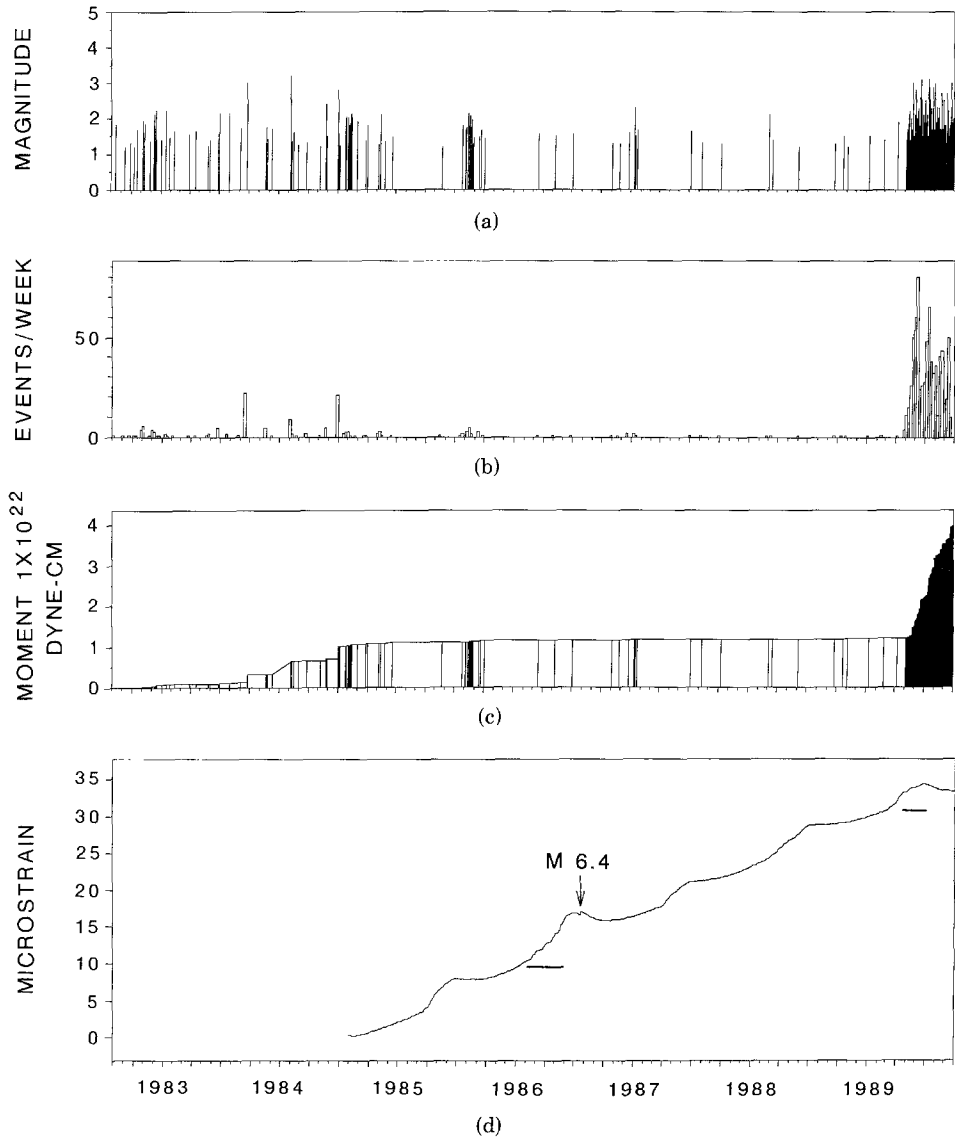


FIG. 2. Time history of Mammoth Mountain seismicity from June 1982 through September 1989. (a) Magnitude of $M \geq 1.2$ events versus time, (b) number of $M \geq 1.2$ events per week versus time, (c) cumulative seismic moment versus time, (d) dilatational strain recorded by the Devils Postpile borehole strainmeter (POPS in Fig. 1). Vertical line indicates time of $M = 6.4$ Chalfant Valley earthquake; short bars indicate intervals of strain transients.

beneath the north flank of Mammoth Mountain to between 4 and 6 km beneath the southwest flank (Profile B-B' in Fig. 3b). Note in particular that the upper 4 km of the crust beneath the southwest flank is nearly aseismic while the seismicity is confined to the upper 4 km of the crust beneath the north flank of the mountain. Note also that the hypocenters form a doughnut-shaped pattern with the central section of the mountain remaining nearly aseismic. This central quiescent volume persists with the current swarm.

Focal mechanisms calculated for well-recorded earthquakes having at least 15 P -wave first-motion observations using the grid search technique of Reasenber

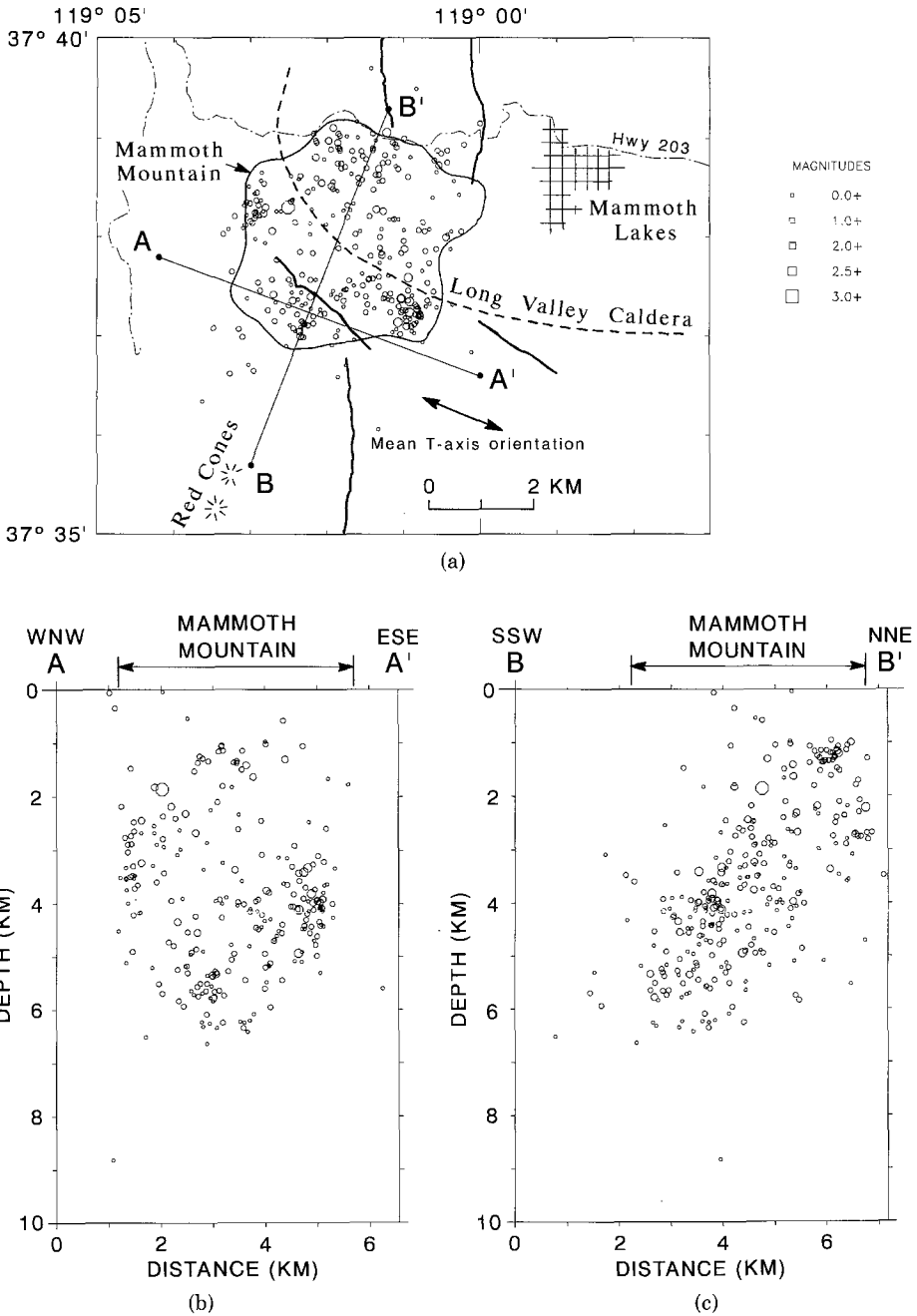


FIG. 3. Seismicity map and depth sections for the 1982 to 1988 Mammoth Mountain activity: (a) epicentral map; double arrow indicates mean *T* axis orientation for earthquake focal mechanisms; (b) depth section with hypocenters in (a) projected onto the plane A-A'; (c) depth section with hypocenters in (a) projected onto the plane B-B'.

and Oppenheimer (1985) show a mix of strike-slip and normal fault plane solutions with a tendency for the *T* axes to cluster about an orientation slightly north of west (Fig. 3). This orientation is consistent with that of the local stress field suggested by the northerly strike of the Mono-Inyo volcanic vents and associated dikes (Eichelberger *et al.*, 1985; Fink, 1985).

CURRENT ACTIVITY

Seismicity

The initial phase of the current swarm developed much like an aftershock sequence in reverse (Fig. 4). Following its onset on 4 May 1989, the activity rate grew with an exponential-like increase peaking on 12 June with some 25 $M \geq 1.2$ events (Fig. 4b). From 12 June through early August, the activity fluctuated about an average rate of five $M \geq 1.2$ events per day with occasional bursts exceeding 20 events per day. The activity rate began to slow through August and September and has since been characterized by brief flurries of $M \leq 2$ events separated by days of

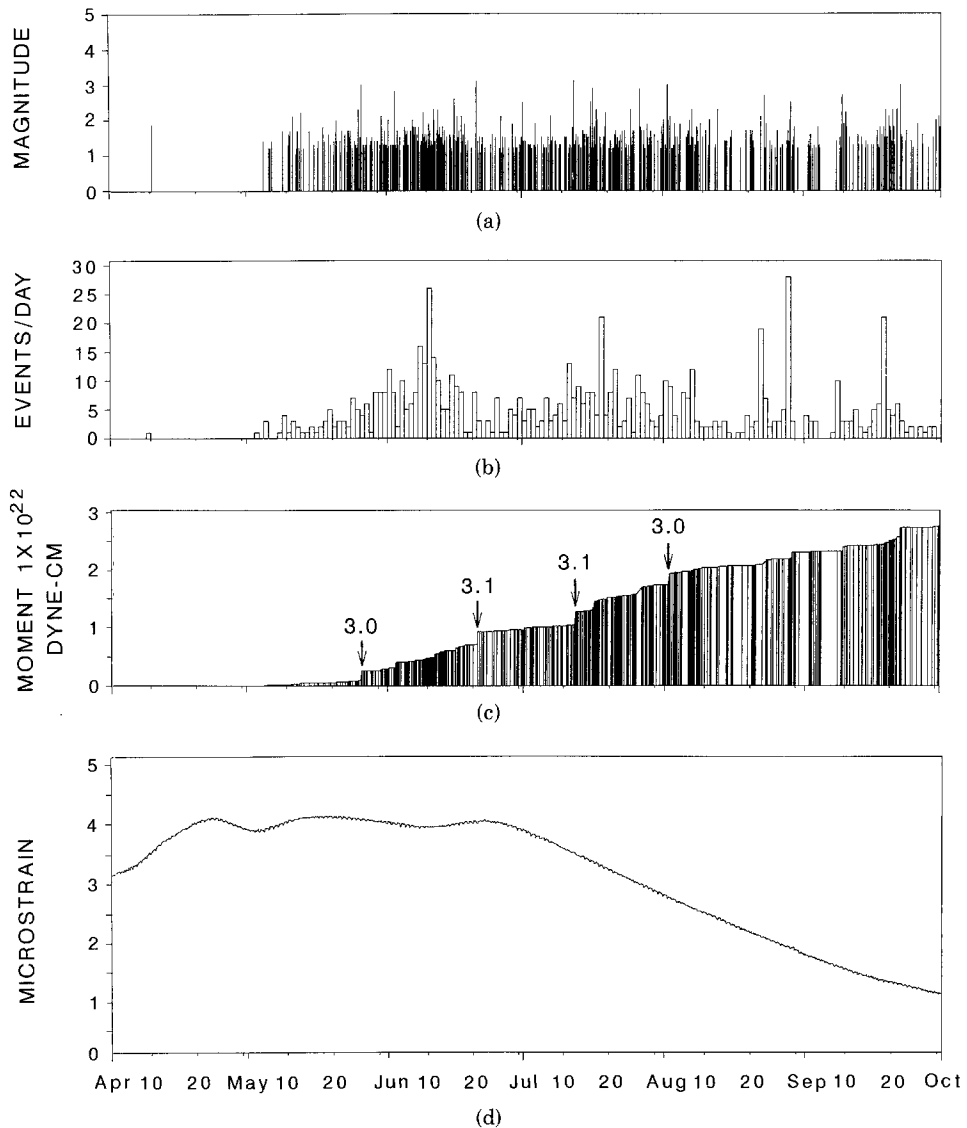


FIG. 4. Time history of the current Mammoth Mountains swarm from April through September 1989: (a) Magnitude of $M > 1.2$ events versus time, (b) rate of $M > 1.2$ events versus time, (c) cumulative seismic moment for all located events ($M \geq 0.5$), with times of $M \geq 3$ events indicated by arrows, (d) dilatational strain recorded by the Devils Postpile strain meter (POPS in Fig. 1) with the long-term linear compressional strain rate of 6.8 microstrain/yr (see Fig. 2d) removed.

relative quiescence. The largest events recorded in the swarm to date include only four $M \approx 3$ earthquakes that occurred on 26 May, 20 June, 12 July, and 1 August. These events stand out in the plot of cumulative seismic moment for the swarm through the end of September (Fig. 4c), and their widely spaced temporal occurrence emphasizes the swarm-like character of this earthquake sequence. The cumulative seismic moment for all located events ($M > 0.5$) in the swarm through the end of September is 2.72×10^{22} dyne-cm, which corresponds to the moment of a single $M \approx 4$ earthquake.

The magnitude distribution for earthquakes under Mammoth Mountain is well-described by a Gutenberg–Richter relation with $b = 1.2 \pm 0.1$ both for the pre-1989 activity and for the current swarm. This elevated b -value is typical for seismicity in volcanic areas and is distinctly higher than the average value of 0.9 found for most of California (Reasenber and Jones, 1989).

The discussion based on Figure 4a and b is restricted to events above the completeness threshold ($M \geq 1.2$) to present a consistent picture of the temporal and statistical properties of the swarm. In fact, the swarm includes a multitude of smaller events. The peak in activity rate on 12 June, for example, included nearly 40 $M \geq 0.5$ events detected and located by the on-line computer systems and several hundred $M > 0$ events recorded on the nearby seismic stations at Mammoth Pass (MMP) and Devils Postpile (MDP).

The epicenters of current swarm earthquakes large enough for reliable locations ($M \geq 0.5$) form a slightly elongate pattern with the long dimension extending from beneath the north edge of the mountain toward the Red Cones 7 km to the south-southeast (Fig. 5a). Most of these epicenters are concentrated in a dense, vaguely Y-shaped cluster beneath the southwest flank of the mountain. One of the north-trending arms of the Y lies beneath central Mammoth Mountain, and the other follows the western margin of the mountain; the tail extends some 2 km south-southwest of the mountain. The east flank of the mountain, which produced minor swarms in 1984 and 1985 (see Fig. 2a) has remained relatively quiet during this current activity.

The corresponding hypocenters occupy roughly the same crustal volume as the earlier swarm activity with the important exception of two newly activated volumes beneath the south flank of the mountain: one at depths less than 3 km and the other at depths extending from 6 to 9 km (compare the cross sections in Figs. 3 and 5). The deeper of these newly activated volumes has a slab-like geometry that is roughly 3 km in breadth and height (profile B–B') but less than 0.5 km in width (profile A–A'). These deep hypocenters, which correspond to the tail in the Y-shaped cluster of epicenters in map view, form a keel beneath the dense concentration of hypocenters at 5 to 6 km that defines the two north-trending arms in the Y-shaped cluster. The shallower newly activated volume developed late in the swarm with a flurry of earthquakes on 29 August at depths less than 3 km beneath the southwest flank of the Mountain.

The remaining, more diffusely distributed hypocenters shallow northward from 4 to 6 km beneath the south flank to less than 4 km beneath the north flank of the mountain (profile B–B'), enclosing an aseismic volume that underlies the west flank of the mountain. This aseismic volume has an ellipsoidal shape that, in map view, is outlined by the northward-branching arms of the Y-shaped cluster and the northeast-trending lineation of epicenters beneath the northwest edge of the mountain. It is capped by the cluster of earthquakes in the upper 3 km of the crust beneath the south flank. The base of this aseismic volume tends to shallow

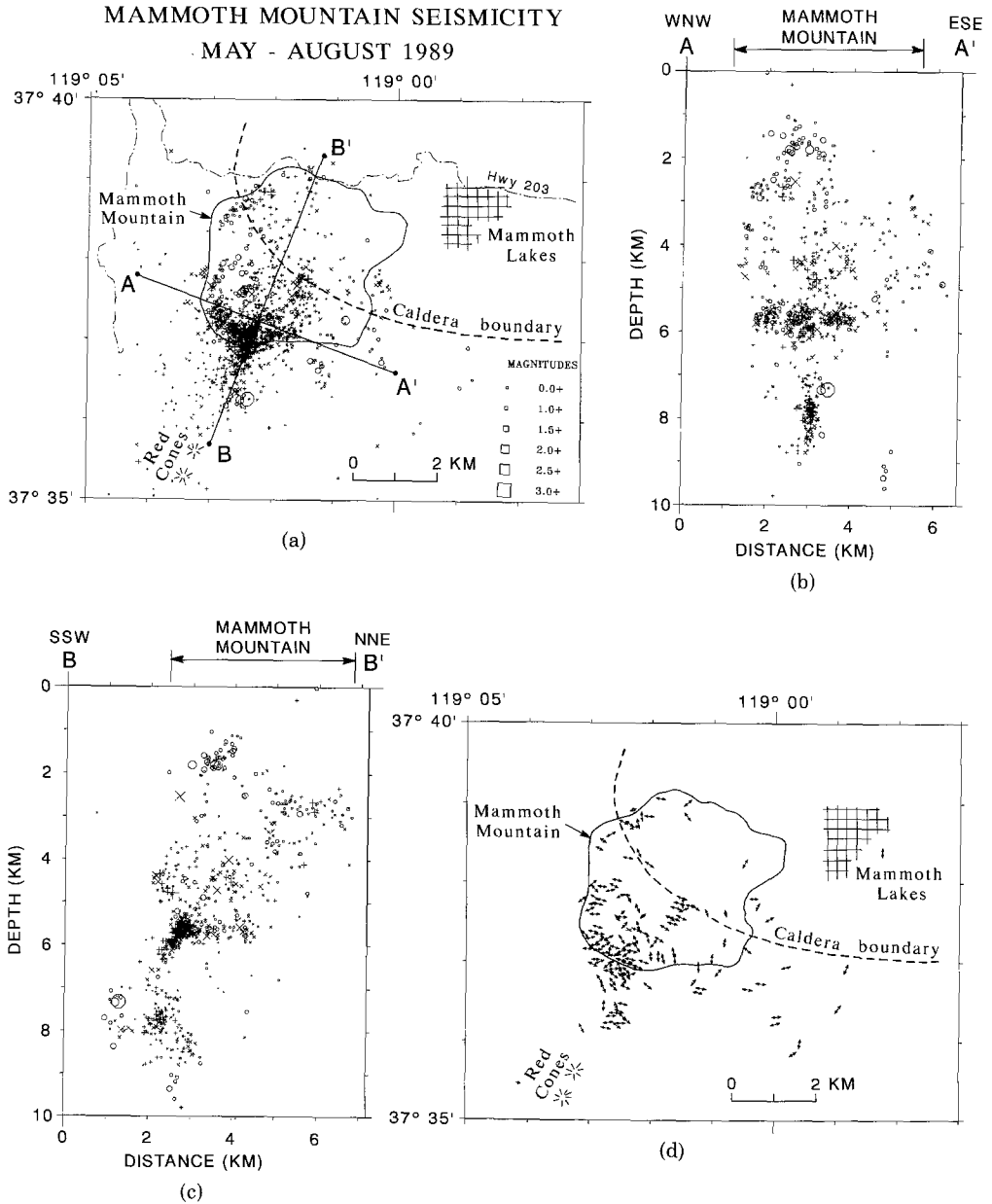


FIG. 5. Seismicity map and cross sections of the 1989 swarm: (a) epicentral map: +, events in May and June; ×, events in July; ○, events in August; (b) depth section with hypocenters in (a) projected onto the plane A-A'; (c) depth section with hypocenters in (a) projected onto the plane B-B'; (d) T-axis orientations of 303 focal mechanisms determined for well-recorded swarm earthquakes.

northward from roughly 5 to less than 4 km, although the paucity of deeper earthquakes beneath the western half of the aseismic volume leaves its base poorly defined here.

The initial swarm activity began on 4 May at depths between 5 and 6 km beneath the southwest flank of the mountain (near the base of the earlier swarm activity and the junction in the Y-shaped cluster). Five days later it deepened to define the keel at depths between 6 and 9 km. Activity continued within this initial, limited

volume through May. In early June, it began expanding at a fairly uniform rate both northward and to shallower depths so that, with the exception of the keel, the entire volume illustrated in Figure 5 had become active with $M \geq 0.5$ events by the end of August (activity in the keel quit rather abruptly during the second week of August). Episodes of increased activity during this period typically began in widely separated sections of the swarm volume at essentially the same time (within an hour or so) suggesting effective hydrolic connectivity throughout the growing swarm volume. During this interval, minimum focal depths for $M \geq 0.5$ events became progressively shallower at a rate of roughly 2 km per month with the mean depth following at a rate of about 1 km per month. This shallowing tendency for $M \geq 0.5$ events culminated in a flurry of $M < 2.5$ events on 29 August at depths less than 3 km beneath the southwest flank of the mountain. Smaller events had been occurring at these shallow depths since at least mid-June, however, as revealed by numerous $M < 0.5$ earthquakes with S - P times less than 0.5 sec recorded on the MMP station just south of the mountain. Although these events were too small for multi-station locations, their short S - P times require that they be located somewhere within the upper 3 km of the crust beneath the southwest flank of the mountain.

We have calculated fault plane solutions for all swarm earthquakes that occurred from 11 May through 16 September with at least 15 P -wave first-motion observations using the Reasenbergs–Oppenheimer (1985) grid search technique. As with the earlier swarms, the resulting set of 303 solutions shows a mix of normal and strike-slip mechanisms with T axes predominantly oriented in a northwest-southeast direction (the mean T -axis orientation for the entire set is approximately N70°W (Fig. 5d)). The T axes for events occurring within the Y-shaped seismicity distribution tend to be perpendicular to local orientations of the arms and tail of the Y. Although we place little weight on any single fault plane solution in this initial analysis, the overall pattern of T -axis orientations seems stable and significant.

Distinctive Earthquakes

Although the majority of swarm earthquakes are indistinguishable from normal “tectonic” earthquakes, a few have distinct characteristics that deserve special attention. The most noteworthy include spasmodic bursts and events enriched in low-frequency energy.

Rapid-fire (spasmodic) bursts of small earthquakes with overlapping coda have occurred virtually daily since early June during this swarm. Individual bursts typically last from tens of seconds to tens of minutes, and in some cases the signal level between clearly identifiable earthquakes remains above background well beyond normal coda decay times (See Fig. 6a). Particularly strong sequences with durations of several minutes occurred on 2 June, 26 June, 6 July, 13 July, 19 July, and 26 July. Similar bursts were recorded during the recurring earthquake swarms in the south moat from mid-1980 through mid-1982 (Ryall and Ryall, 1983) and during earlier Mammoth Mountain swarms from mid-1982 through 1985. Identifiable events within a given burst appear to be generated within essentially the same crustal volume, and they generally have S - P times that range from 0.6 to 1.0 sec at station MMP. The source volume for the burst in Figure 6, for example, appears to be slightly east of the summit of Mammoth Mountain at a depth of about 4 km.

Seismic bursts of the sort illustrated in Figure 6 are seldom observed in purely tectonic environments. Ryall and Ryall (1980) referred to the bursts associated with the recurring south moat swarms as “spasmodic tremor” based on their similarity to tremor-like sequences beneath Kilauea Volcano, Hawaii, described by Eaton

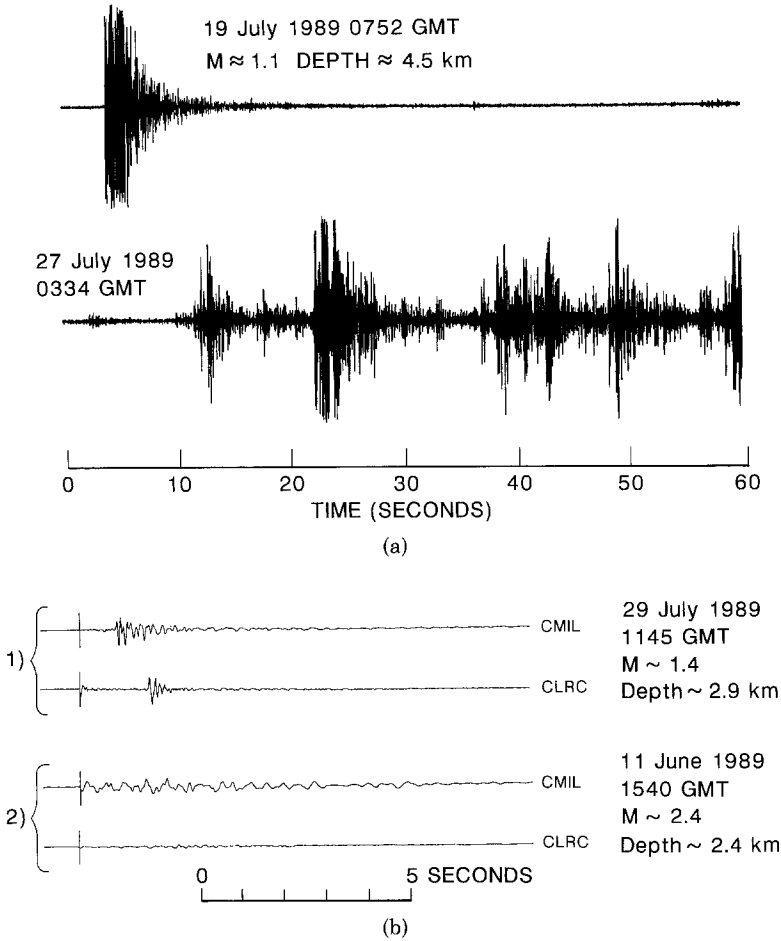


FIG. 6. Examples of selected swarm earthquakes recorded at station MMP (see Fig. 1): (a) typical swarm ($M \approx 1$) earthquake and the onset of a spasmodic burst; (b) seismograms from events recorded on the CDMG stations CMIL and CLRC (see Fig. 1): (1) typical swarm earthquake, and (2) an event with enhanced low-frequency energy.

(1962). These Mammoth Mountain bursts also share many similarities with the onset of intrusion events recorded on Kilauea Volcano (see Fig. 45.3 in Koyanagi *et al.*, 1987). Spasmodic bursts are dominated by brittle failure, however, and are distinct from the monochromatic waveforms of harmonic (volcanic) tremor driven by fluid dynamical processes such as vigorous magma flow or magma degassing at shallow depths. To minimize confusion with harmonic (volcanic) tremor and the implied vigorous involvement of magma in the source process, we use “spasmodic bursts” to describe these sequences of overlapping earthquakes.

The process producing spasmodic bursts remains speculative, but a likely mechanism involves rapid-fire brittle failure along sub-adjacent surfaces driven by a transient increase in local fluid pressure. Niitsuma *et al.* (1985) describe similar sequences in the Takinoue geothermal field (Japan) associated with pressure transients generated by shutdown operations on production wells.

Seismograms from a number of swarm earthquakes show waveforms relatively enriched in low-frequency energy. The seismic system operated by the California Division of Mines and Geology in Sacramento performs automatic, near-real-time

spectral analysis of earthquakes and is specifically designed for the prompt identification of earthquakes deficient in high frequency seismic energy within the caldera that might represent long-period volcanic earthquakes or harmonic tremor (McNutt, 1989). This system identified ten events with low-frequency waveforms in mid-June (seven on 11 June, one 30 July, and two in mid-August) (see example in Fig. 6b). While visually scanning the seismogram films, one of us (A.M.P.) identified two small ($M \approx 1.5$) earthquakes that occurred at 0057 and 0059 hours (GMT) on 20 July at depths of approximately 18 km beneath the west flank of Mammoth Mountain. These events are unusual both because their focal depths are nearly twice as deep as any other earthquake yet recognized beneath Mammoth Mountain and because they also have relatively low frequency waveforms. With the possible exception of the smaller of the deep events on 20 June, however, none of these earthquakes show the nearly monochromatic waveforms typical of long-period volcanic earthquakes as described by Koyanagi *et al.* (1987).

Deformation

The geodetic and deformation monitoring networks in Long Valley caldera are centered on the resurgent dome and south moat where most of the deformation within the caldera has occurred during the last decade (Fig. 1; Hill, 1984). They provide marginal coverage for deformation centered beneath Mammoth Mountain or the southern section of the Inyo-Mono craters volcanic chain. Three of these deformation monitoring systems, however, have shown weak signals that are roughly coincident in time with the current earthquake swarm beneath Mammoth Mountain: (1) the bore-hole dilatometer (POPS) located at the Devils Postpile National Monument just 3 km west of the summit of Mammoth Mountain, (2) the two-color geodimeter network spanning the central section of the caldera, and (3) two L-shaped level arrays within 8 km of Mammoth Mountain.

The bore-hole dilatometer has provided extremely sensitive data on volumetric strain changes in the vicinity of Mammoth Mountain since its installation in 1984 (Fig. 2d; Johnston *et al.*, 1987; Silverman *et al.*, 1989). The strain data for the POPS dilatometer during the period 1 April through 31 August 1989 (Fig. 4d) shows several unusual strain transients through June followed by a gradual extensional trend from July through September. The only other time this instrument recorded similar strain transients was in the months preceding the $M = 6.4$, 21 July 1986, Chalfant Valley earthquake (Fig. 2d). These transients define a subdued M-shaped pattern that begins in early April and persists through the end of June followed by a gradual dilatational excursion through the end of September. The initial hump-shaped transient clearly leads the onset of the earthquake swarm by more than 2 weeks.

The amplitudes of the hump-shaped transients from April through June are only a few tenths of a microstrain; the anomalous dilatational excursion from early July through mid-September amounts to just over 2 microstrain. Preliminary calculations suggest that, if these strain variations are due to dike injection at depths between 3 to 8 km within the seismogenic swarm volume, they result from pressure increases above the least compressive stress of less than 10 bars.

The two-color geodimeter network spanning the south-central section of the caldera (Fig. 1) has shown gradually slowing extension strain across the resurgent dome and south moat based on bi-weekly measurements from mid-1983 through mid-1988 (Langbein, 1989). The extensional strain rate over the last several years has averaged approximately 1×10^{-6} per year, nearly an order of magnitude larger than the 1×10^{-7} resolution afforded by this ranging instrument (Slater and

Higgett, 1976). In late spring of this year around the time of the swarm onset, the network began to show compressional deformation in the N30°E direction while extension continued with little change in the N60°W direction. Because Mammoth Mountain falls outside the network, however, we can only say that, if the observed compressional deformation is due to an inflation source beneath Mammoth Mountain, the inflation rate in that source volume must be less than 0.004 km³/yr and the source must be at least 9 km deep.

None of the telemetered signals from the shallow bore-hole tilt meters operated in the caldera since mid-1982 (Mortensen and Hopkins, 1987) have shown a coherent tilt pattern (above a noise level of a few microradians) that might be associated with the Mammoth Mountain swarm. Two of the eight L-shaped level (dry tilt) figures showed marginal tilt changes that may be related to the swarm activity. These figures are measured approximately four times a year and were reoccupied during the first week of June. The JEE figure on the north flank of Mammoth Mountain showed a marginal (one standard deviation) eastward tilt reversing a pattern of slow westward tilt (0.9 microradians/yr) since early 1984, and the YMCA Figure 7 km east of the mountain showed a somewhat more significant (in excess of two standard deviations) northward tilt reversing a steady southward tilt (2.7 microradians/yr) since mid-1983.

Fumarole Temperatures and Gases

The three recognized areas of thermal-fluid discharge on Mammoth Mountain have shown no significant changes associated with the swarm through the end of September. Two weakly pressurized steam vents are located on the north and south flanks, and a low-chloride hot spring is located near the southwest base. The persistence of the vents and the chemical characteristics of their discharge suggests a relatively shallow heat source beneath the mountain. Gas samples collected in 1982 and 1984 from the north steam vent yielded temperatures of 80° to 90°C, ³He/⁴He ratios (normalized for the ratio in air R_A) of 3.6 to 4.5 (Welhan *et al.*, 1988; G. A. Suemnicht, Unocal Geothermal Division, personal comm., 1989), and a $\delta^{13}\text{C}$ value of -5.6. Helium isotope ratios greater than R_A indicate a mantle or magmatic helium component as does the observed $\delta^{13}\text{C}$ value. A resampling of this vent on 7 July 1989 found that the composition of noncondensable gases and the $\delta^{13}\text{C}$ value had not changed. The helium isotope value for this sample was 3.6 (B. M. Kennedy, University of California, Berkeley, personal comm., 1989). Similarly, the helium isotope ratio for a July 1989 sample from the hot spring near the southwest base of the mountain at Reds Meadow was essentially the same as for a sample collected in 1984 (2.4 and 2.5, respectively).

CONCLUSIONS

The energy involved in this swarm of $M < 3.2$ earthquakes beneath Mammoth Mountain remains small with respect to the May 1980 $M \approx 6$ earthquakes or the recurring swarms of $M \approx 4$ to $M \approx 5$ earthquakes in the south moat from mid-1980 through mid-1983. The cumulative seismic moment from the onset of the current swarm in early May through the end of August corresponds to a single $M \approx 4$ earthquake, and deformation measurements indicate that cumulative strains associated with this activity are on the order of 1×10^{-6} . In spite of its modest cumulative seismic moment and strain energy, however, this swarm holds special interest because of its persistence and evidence for magmatic involvement. In particular, the extended duration and relatively steady activity level that character-

ize this swarm reflect a slow but persistent influx of strain energy into a limited volume of the crust beneath Mammoth Mountain. The evidence listed below points to the intrusion of magmatic fluids into the crust beneath the mountain as the local source of strain energy driving the swarm.

1. The swarm is located at the south end of the youthful Mono-Inyo volcanic chain, which has erupted repeatedly over the last several tens of thousands of years. The southernmost magmatic vent (the Deadman Dome vent) for the eruption 500 to 600 years ago was just 8 km north of Mammoth Mountain, and three small phreatic blasts occurred on the north flank of the mountain at the time of this eruption. These eruptions are presumably fed by a persistent source of magma in the crust somewhere beneath the chain.
2. The earthquake swarm developed with an exponential-like increase in the rate of activity during the first month and was followed by a sustained, quasi-stationary activity level that has persisted for at least 5 months. The onset of the swarm (brittle deformation) followed the onset of a local strain episode by nearly 2 weeks suggesting that the swarm represents a delayed, brittle response to the local, aseismic influx of strain energy into the crust. The distribution of earthquake magnitudes in the swarm is described by a relatively high b -value (1.2) typical of volcanic seismicity.
3. The hypocenters for the swarm earthquakes define a vertical, dike-like keel at depths between 6 and 9 km beneath the shallower, more diffuse cluster of hypocenters. The north-northeast strike of the keel is nearly collinear with that of the north-striking dike that fed the eruption of the Inyo Domes 500 years ago. It is also nearly perpendicular to both the mean orientation of T axes for the swarm earthquakes and to the T axes of earthquakes within the keel. Brittle deformation associated with the keel earthquakes thus involves extension at a high angle to the plane of the keel consistent with dike injection along this plane.
4. The frequent spasmodic bursts associated with this swarm and the less common events deficient in high-frequency energy suggest fluid involvement. We have, however, seen no evidence for vigorous magma transport or degassing in the form of harmonic (volcanic) tremor or the nearly monochromatic waveforms of volcanic low-frequency earthquakes.

Even if this swarm does, as we suspect, represent a magmatic intrusion into the crust beneath Mammoth Mountain, it is unlikely to culminate in an eruption. Evidence from deeply eroded calderas indicates that repeated intrusions of dikes into the shallow crust persist for several million years after caldera collapse and that relatively few of these dikes reach the surface to produce eruptions (Lipman, 1984). In their exhaustive study of historical unrest associated with large calderas throughout the world, Newhall and Dzurisin (1988) document that, although episodes of swarms and ground deformation are common, most do not culminate in volcanic eruptions. Nevertheless, the occurrence of this swarm together with its magmatic signature emphasizes that the magmatic system underlying the Mono-Inyo chain and Long Valley caldera is not dead and that such episodes of unrest have the potential for evolving toward an eruption.

ACKNOWLEDGMENTS

Hypocentral locations for Mammoth Mountain earthquakes from 1982 through 1987 are due to the diligent work of Robert S. Cockerham. We are grateful to Robert Daniel for drawing our attention to

the similarity between spasmodic bursts beneath Mammoth Mountain to the pressure-induced earthquake sequences triggered in the Takinoue geothermal field.

REFERENCES

- Bailey, R. A. (1989). Geologic map of Long Valley caldera, Mono-Inyo craters volcanic chain and vicinity, Mono County, California, U.S. Geological Survey Misc. Inves. Map I-1933.
- Bolt, B. A. and R. D. Miller (1975). Catalog of earthquakes in northern California and adjoining areas 1 January 1910–31 December 1972, Seismographic Station, University of California, Berkeley, 567 pp.
- Cramer, C. H. and T. R. Toppazada (1980). A seismological study of the May 1980, and earlier activity near Mammoth Lakes, California, in Mammoth Lakes, California Earthquakes of May 1980, R. W. Sherburne (Editor), Calif. Division of Mines and Geology Special Report 150, Sacramento, California, 141 pp.
- Eaton, J. P. (1962). Crustal structure and volcanism in Hawaii, in *Crust of the Pacific Basin*, G. A. Macdonald and H. Kuno (Editors), American Geophysical Union Monograph **6**, 13–29.
- Eichelberger, J. C., P. C. Lysne, C. D. Miller, and L. W. Younker (1985). Research drilling at Inyo Domes, California: 1984 results, *EOS* **66**, 186–187.
- Farrar, C. D., M. L. Sorey, S. A. Rojstaczer, C. J. Janik, R. H. Mariner, and M. D. Clark (1985). Hydrologic and geochemical monitoring in Long Valley caldera, Mono County, California, 1982–1984, U.S. Geological Survey Water Resources Invest. Report 85-4183, 137 pp.
- Fink, J. H. (1985). Geometry of silicic dikes beneath the Inyo domes, California, *J. Geophys. Res.* **90**, 11127–11134.
- Hileman, J. A., C. R. Allen, and J. M. Nordquist (1973). Seismicity of the southern California region 1 January 1932 to 31 December 1972, Seismological Laboratory, California Institute of Technology, Pasadena, California, 487 pp.
- Hill, D. P. (1984). Monitoring unrest in a large silicic caldera, the Long Valley-Inyo craters volcanic complex in east-central California, *Bull. Volcanol.* **47**, 371–395.
- Hill, D. P., R. A. Bailey, and A. S. Ryall (1985). Active tectonic and magmatic processes beneath Long Valley caldera, eastern California: a summary, *J. Geophys. Res.* **90**, 11111–11120.
- Johnston, M. J. S., A. T. Linde, M. T. Gladwin, and R. D. Borchardt (1987). Fault failure with moderate earthquakes, *Tectonophysics* **144**, 189–209.
- Koyanagi, R. K., B. Chouet, and K. Aki (1987). Origin of volcanic tremor in Hawaii Part I Data from the Hawaiian Volcano Observatory 1969–1985, in *Volcanism in Hawaii*, U.S. Geol. Surv. Profess. Paper 1350, 1221–1257.
- Langbein, J. (1989). The deformation of the Long Valley caldera, eastern California, from mid-1983 to mid-1988; measurements using a two-color geodimeter, *J. Geophys. Res.* **94**, 3833–3849.
- Lipman, P. W. (1984). The roots of ash flow calderas in the western North America: windows into the tops of granitic batholiths, *J. Geophys. Res.* **89**, 8801–8848.
- Mastin, L. G. and D. D. Pollard (1989). Surface deformation and shallow dike intrusion processes at Inyo Craters, Long Valley, California, *J. Geophys. Res.* **92**, 13221–13235.
- McNutt, S. R. (1989). Analysis of earthquake spectra from Long Valley, California, using the Newt Seismic System, *California Division of Mines and Geology Open-File Rept.* 89-6, 48 pp.
- Miller, C. D. (1985). Holocene eruptions at the Inyo volcanic chain, California: implications for possible eruptions in the Long Valley caldera, *Geology* **13**, 14–17.
- Mortensen, C. E. and D. G. Hopkins (1987). Tiltmeter measurements in Long Valley caldera, California, *J. Geophys. Res.* **92**, 13767–13776.
- Newhall, C. G. and D. Dzurisin (1988). Historical unrest at large calderas of the world, *U.S. Geological Survey Bull.* 1855, 1108 pp.
- Niitsuma, H., K. Nakatsuka, N. Chubachi, H. Yokoyama, and M. Takanoishishi (1985). Acoustic emission measurement of geothermal reservoir cracks in the Takinoue (Kakkonda) field, Japan, *Geothermics* **14**, 525–538.
- Pitt, A. M. and D. W. Steeples (1975). Microearthquakes in the Mono Lake-Northern Owens Valley, California region from September 28 to October 18, 1970, *Bull. Seism. Soc. Am.* **65**, 835–844.
- Reasenber, P. A. and L. M. Jones (1989). Earthquake hazard after a mainshock in California, *Science* **243**, 1173–1176.
- Reasenber, P. A. and D. H. Oppenheimer (1985). FPFIT, FPLOT and FPPAGE: Fortran computer programs for calculating and displaying earthquake fault-plane solutions, *U.S. Geol. Surv. Open-File Rept.* 85-739, 109 pp.
- Rison, W., J. A. Welham, R. Poreda, and H. Craig (1983). Long Valley: increase in the $^3\text{He}/^4\text{He}$ ratio from 1978 to 1983, *EOS* **64**, 891.

- Rundle, J. B. and D. P. Hill (1988). The geophysics of a restless caldera--Long Valley, California, *Ann. Rev. Earth Planet. Sci.* **16**, 251-271.
- Ryall, A. and F. Ryall (1983). Spasmodic tremor and possible magma injection in Long Valley caldera, eastern California, *Science* **219**, 1432-1433.
- Savage, J. C. and M. M. Clark (1980). Magmatic resurgence in Long Valley caldera, California: possible cause of the 1980 Mammoth Lakes earthquakes, *Science* **217**, 531-533.
- Sieh, K. and M. Bursik (1986). Most recent eruption of the Mono Craters, east-central California, *J. Geophys. Res.* **91**, 12,539-12,571.
- Silverman, S., C. Mortensen, and M. J. S. Johnston (1989). A satellite-based digital data system for low-frequency geophysical data, *Bull. Seism. Soc. Am.* **79**, 189-198.
- Slater, L. E. and G. R. Higgett (1976). A multi-wavelength distance-measuring instrument for geophysical experiments, *J. Geophys. Res.* **81**, 6299-6306.
- Smith, G. M. and F. S. Ryall (1980). Bulletin of the Seismological Laboratory for the Period January 1, 1975 to December 31, 1979, Mackay School of Mines, Univ. of Nevada, Reno, 84 pp.
- Steeles, D. W. and A. M. Pitt (1975). Microearthquakes in and near Long Valley, California, *J. Geophys. Res.* **81**, 841-847.
- Welhan, J. S., R. J. Poreda, W. Rison, and H. Craig (1988). Helium isotopes in geothermal and volcanic gases of the western United States. II. Long Valley caldera, *J. Volcanol. Geothermal Res.* **34**, 201-209.

U. S. GEOLOGICAL SURVEY
 345 MIDDLEFIELD ROAD
 MENLO PARK, CALIFORNIA 94025
 (D.P.H., W.L.E., M.J.S.J., J.O.L.,
 D.H.O., A.M.P., P.A.R., M.L.S.)

CALIFORNIA DIVISION OF MINES AND GEOLOGY
 630 BERCUT DRIVE
 SACRAMENTO, CALIFORNIA 95814
 (S.R.M.)

Manuscript received 25 November 1989